

COMPOSITIONAL VARIATION OF Co-RICH PENTLANDITE: RELATION TO THE EVOLUTION OF THE UPPER ZONE OF THE WESTERN BUSHVELD COMPLEX, SOUTH AFRICA

ROLAND K.W. MERKLE AND GERHARD VON GRUENEWALDT

Institute for Geological Research on the Bushveld Complex, University of Pretoria, Hillcrest, Pretoria 0002, Republic of South Africa

ABSTRACT

The uppermost 1200 m of the upper zone of the western Bushveld Complex at Bierkraal were investigated by whole-rock geochemistry and mineral chemistry of olivine and sulfides. The rocks are depleted in Ni, owing to olivine crystallization and separation of immiscible sulfide melt throughout most of the upper-zone sequence. This resulted in a high Co/Ni ratio in the sulfide melt and produced cobalt-rich pentlandite on cooling. Some of the pentlandite is not stoichiometric; no systematic relation between departure from stoichiometry and metal contents or metal ratios is detectable. Variation of Co/Ni in pentlandite is reflected by Co/Ni in coexisting pyrrhotite and in whole-rock compositions. The upper zone does not represent an uninterrupted differentiation of a homogeneous melt. Replenishment by less differentiated magma is reflected in cyclic changes in whole-rock chemistry, and in pentlandite and olivine compositions. The position of layers of magnetite at the base of geochemical cycles strongly indicates a genetic link between the formation of magnetite layers and magma mixing.

Keywords: pentlandite, Bushveld Complex, upper zone, differentiation, olivine, layers of magnetite, magma mixing, South Africa.

SOMMAIRE

Les 1200 m supérieurs de la zone supérieure du Complexe de Bushveld à Bierkraal ont été étudiés par la géochimie (de la roche entière) et la cristallogéochimie (de l'olivine et des sulfures). Les roches sont appauvries en Ni, étant donné la cristallisation de l'olivine et la séparation d'un liquide sulfuré immiscible dans presque toute la série de la zone supérieure. Comme résultat, on note le rapport élevé Co/Ni dans le bain sulfuré ainsi que la formation de pentlandite riche en cobalt, au refroidissement. Une partie de la pentlandite n'est pas stoechiométrique; nulle relation systématique n'est décelable entre l'écart à la stoechiométrie et la teneur en métaux ou les rapports entre métaux. La variation du rapport Co/Ni dans la pentlandite se reflète dans la valeur dudit rapport dans la pyrrhotite coexistante et dans la composition de la roche entière. La zone supérieure ne représente pas la différenciation d'un bain fondu homogène. La venue d'un magma moins différencié se reflète dans des modifications cycliques dans le chimisme de la roche entière, ainsi que dans la composition de la pentlandite et de l'olivine. La position de couches de magnétite à la base des cycles géochimiques donne une forte indi-

cation de l'existence d'un lien génétique entre la formation des couches de magnétite et le mélange de magmas.

(Traduit par la Rédaction)

Mots-clés: pentlandite, Complexe de Bushveld, zone supérieure, différenciation, olivine, couches de magnétite, mélange de magmas, Afrique du Sud.

INTRODUCTION

The importance of the state of evolution of the magma on the formation of economic and subeconomic sulfide mineralization in the Bushveld Complex is the subject of ongoing research. In the eastern Bushveld Complex, the upper zone shows a systematic change in modal proportions of sulfide minerals as a consequence of magmatic differentiation (Von Gruenewaldt 1976). Most members of the standard assemblage of magmatic sulfides (chalcopyrite, cubanite and pentlandite) evolved on cooling from the monosulfide solid-solution. As no extensive solid-solution series exists in the pure Cu-Fe-S system at low temperature, differentiation will only be reflected in the modal proportions of the sulfides. Differentiation, however, not only influences the bulk composition of the sulfides, but also produces a continuous compositional change in certain sulfide minerals.

During microscope investigations of the sulfides in the upper zone of the western Bushveld, the optical properties (e.g., color, reflectivity) were found to vary with the Co/Ni ratio in pentlandite. As Co and Ni behave differently during differentiation (Irving 1978) and the separation of an immiscible sulfide melt (MacLean & Shimazaki 1976, Rajamani & Naldrett 1978), it was decided to investigate the extent to which changes in pentlandite composition can be related to petrological processes in the highly evolved melt of the upper zone. In addition, it was hoped that the generation of a comprehensive and internally consistent data-base of pentlandite compositions with different contents of Co would provide information on pentlandite stoichiometry and the evolutionary trend of pentlandite compositions in highly differentiated magmatic rocks.

GEOLOGICAL BACKGROUND

In 1974, the Geological Survey of South Africa drilled 3 boreholes on the farm Bierkraal in the Layered Suite of the western Bushveld Complex (Fig. 1). The 3 holes (BK-1 to BK-3) intersected the complete upper zone from the Main Magnetite Layer to the roof contact (against metasediments and granite). Rock types are mainly ferrogabbro, ferrodiorite, anorthosite and magnetite (Walraven & Wolmarans 1979). The data presented in this paper all pertain to the BK-1 core, which penetrated the upper 1200 m of the upper zone (Fig. 2). An important characteristic of the upper zone of the western Bushveld, in contrast to the eastern Bushveld, is the presence of olivine throughout most of the stratigraphic succession.

SAMPLING AND ANALYTICAL PROCEDURE

From the BK-1 core, 139 samples with an average spacing of less than 10 m were taken for analysis. An additional 90 powdered samples of the uppermost 400 m of the upper zone from the same borehole were made available by Dr. R.G. Cawthorn.

Whole-rock major-element contents of 139 samples were obtained at the University of Pretoria by XRF, using standard techniques of preparation (Norrish & Hutton 1969). Whole-rock trace-element concentrations for Co, Cu, Ni, Zn, Zr, Nb, Rb, Sr, Ba and Y of 217 samples were obtained by using pressed-powder briquettes. These were analyzed with multichannel wavelength-dispersion XRF equipment at the Geological Survey of South Africa by courtesy of Dr. C. Frick.

Sulfur contents were determined in all samples using a LECO CS244 infrared-absorption spectrometer with a HF100 induction furnace (housed at the Geological Survey) in an oxygen stream at 1200 - 1400°C. Results were confirmed with a gas chromatograph. A microscope investigation of the remaining slags showed that the rock powder was completely melted, and that volatilization of the sulfur presumably was complete. The lower limit of detection for sulfur (3-sigma level) was calculated to be 3 ppm, using the accelerator as a blank. Based on 7 to 10 replicate analyses, reproducibility (1 sigma) was determined to be 2 ppm at 18 ppm, 16 ppm at 330 ppm, 61 ppm at 3200 ppm and 400 ppm at 2.37 weight %. LECO reference steel was used as a standard.

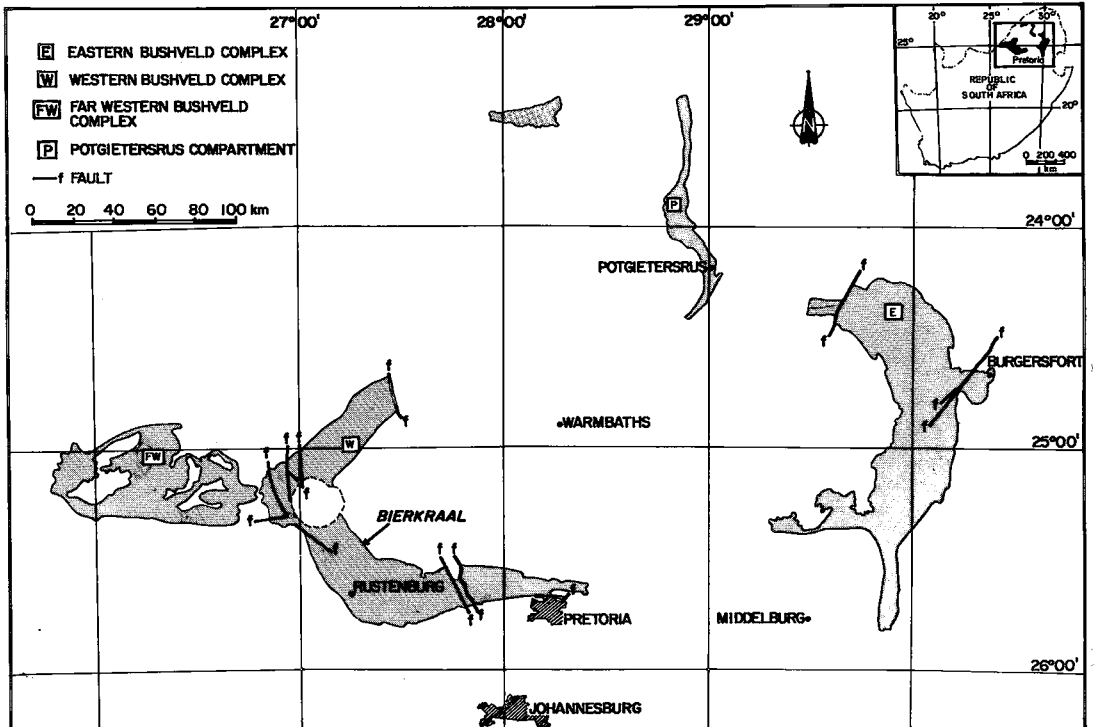


FIG. 1. Position of the Bierkraal drillhole in relation to the general outline of the layered sequence of the Bushveld Complex.

OBSERVATIONS AND ANALYTICAL RESULTS

Immiscible sulfide liquid separated from the silicate melt during crystallization of a large part of the upper zone. A large portion of the sulfide is situated in intergranular spaces; however, drop-like inclusions of sulfides in silicates and oxides are com-

The ore-microscope investigation of the core is based on 252 polished thin sections. Electron-microprobe analyses were carried out with a JEOL 733 Superprobe (with 4 spectrometers) at the University of Pretoria. Sulfides were analyzed for S, Co, Cu, Fe and Ni. As and Zn concentrations in pentlandite and pyrrhotite are below the detection limit. The following standards were used: natural troilite for S and Fe, natural arsenopyrite for As, synthetic cobalt-pentlandite for Co, natural chalcopyrite for Cu, natural millerite for Ni, and synthetic sphalerite for Zn. Acceleration potential was 15 kV with a beam current of 5×10^{-8} A, measured and monitored on a Faraday cup. For full ZAF corrections, the program FZAFM was used. Counting time for each element was 50 seconds, resulting in lower limits of detection (3 sigma) of 200 ppm for Co and 220 ppm for Ni in pyrrhotite. Reproducibility was controlled on a routine basis by calculating the standard deviation from double analyses of identical spots with the formula given by Kaiser & Specker (1956). Calculated reproducibilities s (1 sigma) are given in brackets after the approximate range on which the calculations are based (all values in atomic %). Reproducibility for pyrrhotite was: S, 50 to 53.3 (0.097); Fe, 46.7 to 50 (0.095); Co, 0.04 to 0.09 (0.005 to 0.008); and Ni, 0.02 to 0.03 (0.004). For pentlandite, reproducibility was found to be: S, 47 (0.099); Fe, 5 to 24 (0.047 to 0.102); Co, 8 to 46 (0.058 to 0.144); and Ni, 2 to 21 (0.038 to 0.137).

Depending on the frequency and size of pentlandite in a particular sample, either all grains present or at least 10 big grains were analyzed. Up to 30 spot analyses were made on pyrrhotite coexisting with pentlandite. The results presented in this paper are based on a total of 1306 pentlandite and 3133 pyrrhotite analyses.

Olivine was analyzed at 20 kV and 2×10^{-8} A using pure oxides as standards for Al, Si, Mg, Ti, Mn and Fe, Arenal hornblende (Jarosewich *et al.* 1979) for Ca, natural millerite for Ni and synthetic cobalt-pentlandite for Co. Counting time was 20 seconds except for Al, Co and Ni, where counting time was extended to 50 seconds. The lower limits of detection (3 sigma) in the iron-rich olivine were calculated to be 120 ppm for Co and 160 ppm for Ni. Reproducibility (1 sigma) for the 524 olivine analyses carried out was also estimated from duplicate analyses and was found to be 0.0027 for the $Mg/(Mg + Fe)$ atomic ratio and 57 ppm for cobalt concentration. If a standard deviation of the analyses of more than 3 times the reproducibility is taken as the criterion to reject homogeneity of olivine in a grain or sample, all samples except from 1112.7 m depth in borehole BK-1 can safely be treated as being homogeneous in their forsterite and cobalt contents.

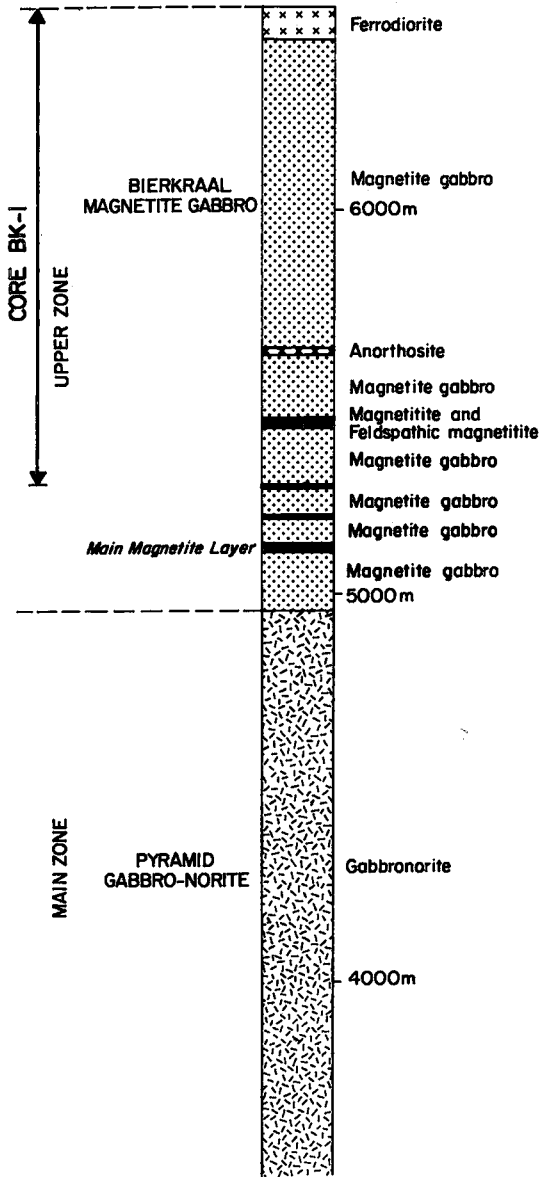


FIG. 2. Simplified stratigraphy of the upper zone of the western Bushveld Complex (modified after SACS 1980) and the stratigraphic succession covered by the BK-1 drill core.

TABLE 1. COBALT CONTENT (ATOMIC %) AND Co/Ni RATIO (ATOMIC) OF PENTLANDITE COMPOSITIONS FROM THE UPPER ZONE

Depth	Co				Co/Ni				N
	x	s	Min	Max	x	s	Min	Max	
440.5 m	34.84	0.32	34.53	35.21	4.84	0.13	4.65	4.91	4
538	38.30	1.62	36.05	40.16	7.91	1.14	6.20	8.97	12
551.5 m	44.08	0.63	43.43	44.66	43.88	0.39	43.37	44.32	4
563.5 m	42.01	0.13	41.83	42.12	21.39	5.09	16.97	25.94	4
581.5 m	43.50	1.31	41.85	46.43	16.82	4.40	12.06	26.86	29
589.5 m	40.95	2.49	31.85	45.46	12.05	3.08	7.70	25.19	94
607.5 m	28.45	2.14	22.69	32.60	2.64	0.47	1.75	3.70	59
620.5 m	28.22	2.46	23.30	34.25	2.28	0.57	1.70	4.32	30
638	20.63	2.60	16.60	25.39	1.55	0.40	1.03	2.29	44
726	43.84	1.60	41.84	45.73	20.81	9.09	11.76	35.11	8
757.5 m	29.46	2.41	22.00	34.12	2.86	0.45	2.13	3.86	91
772.5 m	18.62	3.30	13.27	23.59	1.25	0.35	0.74	1.94	133
798	26.66	0.49	23.92	25.21	1.89	0.06	1.78	1.98	12
810.5 m	24.80	0.50	24.13	25.64	1.78	0.08	1.65	1.89	12
822.8 m	17.43	4.05	12.52	28.20	1.08	0.40	0.67	2.33	87
893	29.28	1.86	27.32	32.72	2.91	0.66	2.34	4.33	12
899	30.16	0.18	29.92	30.31	2.99	0.11	2.99	3.00	4
940.1 m	34.57	0.26	34.31	34.94	4.58	0.12	4.43	4.73	4
951	29.08	1.15	28.16	30.96	2.77	0.31	2.51	3.23	10
968.9 m	28.55	2.57	23.48	31.03	3.83	0.57	1.95	3.72	15
999.8 m	29.82	2.79	24.51	35.58	3.24	0.83	1.90	4.99	46
1009.6 m	31.30	1.74	29.18	35.03	3.38	0.58	2.80	4.90	33
1019.8 m	42.85	1.45	40.92	44.86	17.06	3.37	13.02	22.80	12
1030	40.86	0.74	39.41	41.86	12.15	2.05	8.27	15.80	18
1040.2 m	34.28	3.78	26.72	40.17	5.59	2.71	2.36	11.67	30
1050.2 m	41.81	1.43	39.54	44.45	14.10	5.91	8.84	30.78	34
1060.3 m	42.14	1.30	39.42	44.24	17.64	4.53	10.39	26.30	50
1068.9 m	37.52	2.75	30.84	39.70	15.21	4.41	10.84	21.29	16
1082.2 m	36.19	1.30	34.28	37.85	10.50	2.03	7.35	12.82	11
1086.7 m	37.81	0.65	36.61	38.80	13.32	1.60	9.59	14.97	14
1089.8 m	37.49	1.48	35.67	40.10	9.09	2.30	6.43	13.40	22
1091	37.82	1.54	35.96	40.50	11.07	1.93	8.51	14.14	13
1096.3 m	34.19	2.31	28.53	38.58	7.24	2.61	3.47	14.68	64
1100.8 m	29.06	5.63	20.63	37.00	4.83	2.93	1.57	9.86	34
1103.7 m	25.14	9.54	15.91	33.14	3.22	1.52	1.24	6.44	90
1112.7 m	24.30	6.72	11.98	46.03	3.49	7.95	0.57	40.25	79
1113.4 m	25.56	4.46	19.37	33.45	2.62	1.10	1.39	4.93	30
1117	12.08	3.02	8.78	19.97	0.70	0.30	0.42	1.63	72

x arithmetic mean, s standard deviation, Min lowest value observed, Max highest value observed, N number of analyses. More detailed information is available from the authors on request.

mon. The sulfide mineralogy in the upper zone of the western Bushveld at Bierkraal is at first glance very uniform. It resembles what is normally expected to have crystallized from a sulfide melt that unmixed from a highly evolved silicate melt constantly depleted in highly chalcophile elements, *i.e.*, it consists predominantly of pyrrhotite with only small amounts of chalcopyrite and minor pentlandite. Rare sulfides are sphalerite, molybdenite, loellingite, safflorite, cobaltite, mackinawite, valleriite, pyrite, marcasite, galena and cubanite. Sphalerite, molybdenite, arsenides and galena increase toward the roof of the complex and reflect the enrichment of Zn, Mo, As and Pb in the magma with progressive fractional crystallization. Modal proportions of pyrrhotite, pentlandite and chalcopyrite vary with stratigraphic

position and reflect the variations of whole-rock content of S, Co, Ni and Cu. Sulfides in proximity of layers of magnetite tend to contain a much higher modal proportion of chalcopyrite.

Mineral chemistry

Pentlandite: Although pentlandite occurs in all the sulfide-bearing rocks of the upper zone, amount and size of grains in the topmost 400 m are so small that proper documentation of compositional trends over the entire succession is not possible. Consequently, emphasis was placed on a 225-m-thick succession of rocks between 890 and 1117 m.

In the BK-1 samples only pentlandite with a substantial content of Co was found. The pentlandite is granular in most cases and occasionally displays crystal faces. Fully idiomorphic pentlandite is rare and restricted to compositions with a high content of Co. However, even the most Co-rich grains are not necessarily idiomorphic. In most sulfide ores, flame-like pentlandite exsolutions in pyrrhotite are, apart from granular pentlandite, the most common known form and indicate exsolution at low temperatures (Kelly & Vaughan 1983, Durazzo & Taylor 1982). In the upper zone at Bierkraal, however, only one sample (depth 620 m) contains pyrrhotite with flame-like exsolution lamellae of pentlandite. Formation and preservation of these pentlandite flames are thought to be related to a much stronger hydrothermal alteration at 620 m than in the other samples. Pentlandite grains are generally below 5 μm in diameter and rarely exceed 15 μm . Because of the low bulk concentration of Ni and Co, the total amount of pentlandite in the rock is generally small, rarely exceeding 15 grains per section, even in the most sulfur-rich samples. Pentlandite may occasionally be present in sulfide inclusions in olivine or clinopyroxene, but most frequently occurs in intercumulus patches of sulfide. Pentlandite is readily altered to minerals of the linnaeite group or to disulfides, but despite the hydrothermal alteration of some of the silicates, the pentlandite was not found to be affected.

In the literature, Co-rich pentlandite has been described from serpentinized ultramafic rocks (*e.g.*, Harris & Nickel 1972, Misra & Fleet 1973), from hydrothermal veins (*e.g.*, Petruk *et al.* 1969), and from metamorphosed massive-sulfide ores (*e.g.*, Kouvo *et al.* 1959, Huhma & Huhma 1970, Lindahl 1973, Vaasjoki *et al.* 1974). The occurrence of Co-rich pentlandite of magmatic origin in the Bushveld therefore offers a unique opportunity to investigate the changes of pentlandite composition in relation to changes in bulk-rock chemistry due to magmatic differentiation. The concentration of Co determined and the Co/Ni ratio for the samples investigated are listed in Table 1; a more detailed listing of the

TABLE 2. REPRESENTATIVE COMPOSITIONS* OF PENTLANDITE

Depth	S	Fe	Ni	Co	Total
551.5 m	33.86	7.82	1.31	57.94	100.93
893	33.69	16.81	15.17	35.67	101.34
1009.6 m	33.16	16.20	13.00	38.44	100.80
1040.2 m	33.83	17.67	12.41	37.00	100.91
1040.2 m	33.03	14.06	9.02	44.93	101.04
1060.3 m	32.78	10.80	2.82	54.19	100.59
1082.2 m	33.09	14.42	3.78	48.61	99.90
1082.2 m	32.86	16.64	4.88	45.49	99.87
1100.8 m	33.14	23.30	12.06	30.54	99.04
1103.7 m	33.28	27.75	14.06	23.78	98.87
1112.7 m	32.35	26.22	25.18	15.54	99.29

* in weight %.

analytical results is available from the authors on request. Some examples of compositions with different contents of Co and cation ratios in pentlandite are given in Table 2.

Figures 3 and 4 summarize the Co content determined and the Co/Ni ratio in pentlandite graphically, and allow comparison with the compositional trends of pyrrhotite, olivine, and the whole-rock Co/Ni ratio. The pentlandite displays significant changes in composition with stratigraphic height. The trend

is interrupted by reversals, so that a cyclic pattern in the Co content of pentlandite can be recognized; the most obvious one is developed between 890 m and 1117 m in borehole BK-1. Higher up in the sequence, trends of Co enrichment can be recognized; however, the cyclic pattern is not as evident, owing to rock sequences in which pentlandite grains were not found or are too small to analyze.

Riley (1977) summarized analytical data on pentlandite from the literature and found two different trends of cobalt substitutions: one is restricted to ser-

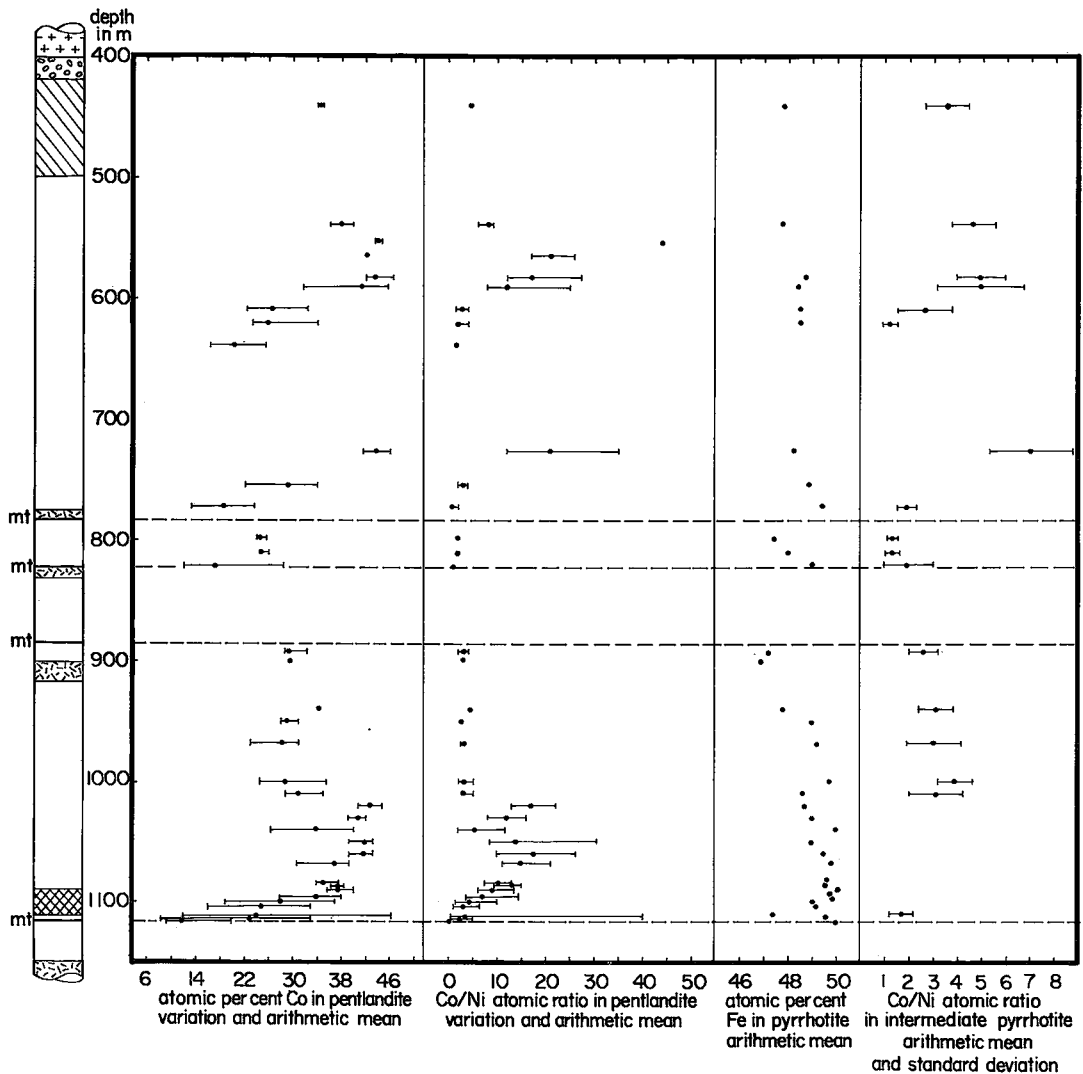


FIG. 3. The total variation and arithmetic means of Co content (in atomic %) and Co/Ni ratios (atomic) in pentlandite in the topmost 700 m of the upper zone at Bierkraal. Also presented are the arithmetic means of Fe contents (in atomic %) and arithmetic means and 1 standard deviation of the Co/Ni ratio (atomic) of pyrrhotite coexisting with pentlandite.

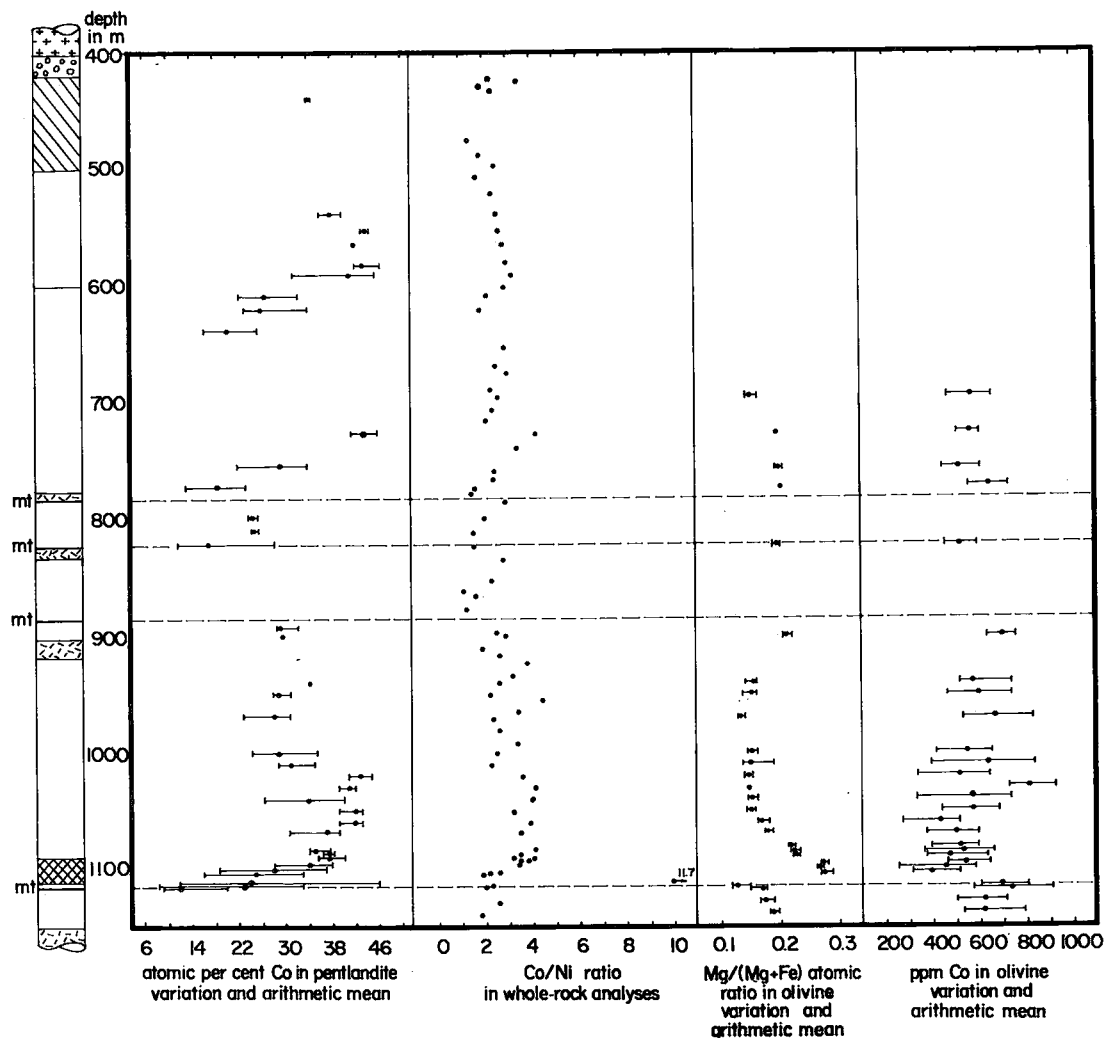


FIG. 4. Comparison of the Co content in pentlandite (see Fig. 3) with the Co/Ni ratio in the whole rock, the total variation and arithmetic mean of the Mg/(Mg + Fe) atomic ratio in olivine, and the total variation and arithmetic mean of Co concentration in olivine.

pentinites and hydrothermal veins, where Co substitutes for Fe; in the other, a feature of metamorphosed massive-sulfide ores in Scandinavia, Co replaces Ni. Cobalt-rich pentlandite from the Bushveld also follows a trend of preferential replacement of Ni (Fig. 5). However, because of the very high Fe/Ni ratio in rocks of the upper zone, this trend is set off toward higher Fe/Ni values than the trend from published data (Fig. 6).

The analyses of the pentlandite show that in the upper zone, the pentlandite is consistently Co-rich. The lowest observed value is 8.2 atomic %, the highest, 46.4, and the overall mean, 28.7 atomic % (Fig. 7). This high content of cobalt is seen as the

reason for the virtual absence of exsolution flames of pentlandite in pyrrhotite. Co increases the upper thermal stability-limit of pentlandite (Vaasjoki *et al.* 1974), so that exsolution of cobalt-rich pentlandite from the monosulfide solid-solution starts at higher temperature than for Co-poor pentlandite. The higher rates of diffusion at elevated temperature would favor granular exsolution. It also seems that cobalt-rich pentlandite has a much stronger tendency toward idiomorphism than ordinary Fe-Ni-pentlandite, so that flame-like exsolution lamellae (which might have formed in analogy to normal pentlandite) could have recrystallized to minute granular grains during the slow cooling of the Bushveld.

During the analyses of pentlandite from the Bushveld, it became obvious that individual grains deviate considerably from the assumed stoichiometric formula of Me_9S_8 , although the mean value of 47.12 atomic % sulfur for all compositions (Fig. 8) was found to be very close to the theoretical value (47.06). It has previously been assumed that a relation between metal ratios and sulfur contents in Co-poor pentlandite might exist (Rajamani & Prewitt 1973). In contrast, Page (1972), Harris & Nickel (1972), and Riley (1977) did not observe a systematic variation in the extent of nonstoichiometry in pentlandite. This, however, could be due to relatively large analytical errors or inconsistencies in the analytical procedure for the data compiled from the literature. The analytical data in this paper are consistent within the analytical reproducibility given above.

To rule out analytical problems as the reason for deviations toward anomalously low contents of sulfur, some nonstoichiometric grains were re-analyzed. The results were found to be reproducible within the expected limits of analytical uncertainty. Analyses with high values of sulfur might have accidentally been influenced by the pyrrhotite surrounding the small grains of pentlandite. If this were the case, then a correlation between Fe content in the pentlandite and the S content should result. Table 3 gives the Spearman correlation matrix for the metals, the metal ratios and sulfur in atomic proportions. No relation between sulfur and iron can be detected. Figures 9A to C also demonstrate that there is no specific reason for nonstoichiometry in cobalt-rich pentlandite.

Pyrrhotite: In the samples investigated, the pyrrhotite consists essentially of mixtures of varying amounts of intermediate pyrrhotite (Morimoto *et al.* 1975) and troilite, resulting in a bimodal frequency-distribution of the iron content, as determined with the microprobe. Some pyrrhotite compositions with different contents of iron are given in Table 4. Because of this bimodal distribution of iron contents, the arithmetic means for pyrrhotite coexisting with pentlandite (Fig. 3) in different samples cannot be compared quantitatively. They do, however, indicate differences in the average content of iron in the pyrrhotite between samples. The concentrations of Co and Ni in this pyrrhotite depend linearly on the iron content and are lowest in troilite, with Ni contents generally below the limit of detection (Merkle, in prep.). Consequently, in order to allow comparison of the Co/Ni ratio of pyrrhotite with that in pentlandite, only intermediate pyrrhotite compositions, with an iron content of 47.8 ± 0.3 atomic %, were selected. These data pertain to the composition of the most iron-rich intermediate pyrrhotite and the interval where 99.7% (3 sigma) of all analyses of pyrrhotite with this composition can be expected.

Only 667 out of 3133 pyrrhotite compositions fall into the required interval of composition, and of these only 354 contain Ni in detectable amounts. Because only pyrrhotite coexisting with pentlandite was included in this study, and because at some levels (mainly above magnetite layers) none of the pyrrhotite could be used because of its high content of Fe,

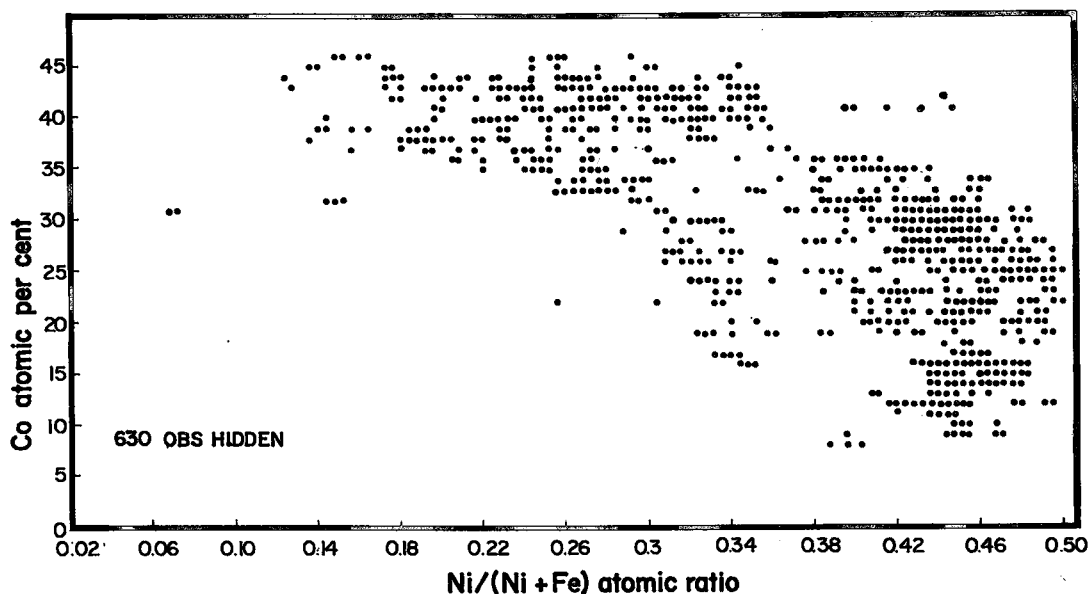


FIG. 5. Variation of the Ni/(Ni + Fe) atomic ratio with increasing Co concentration in the pentlandite from the upper zone.

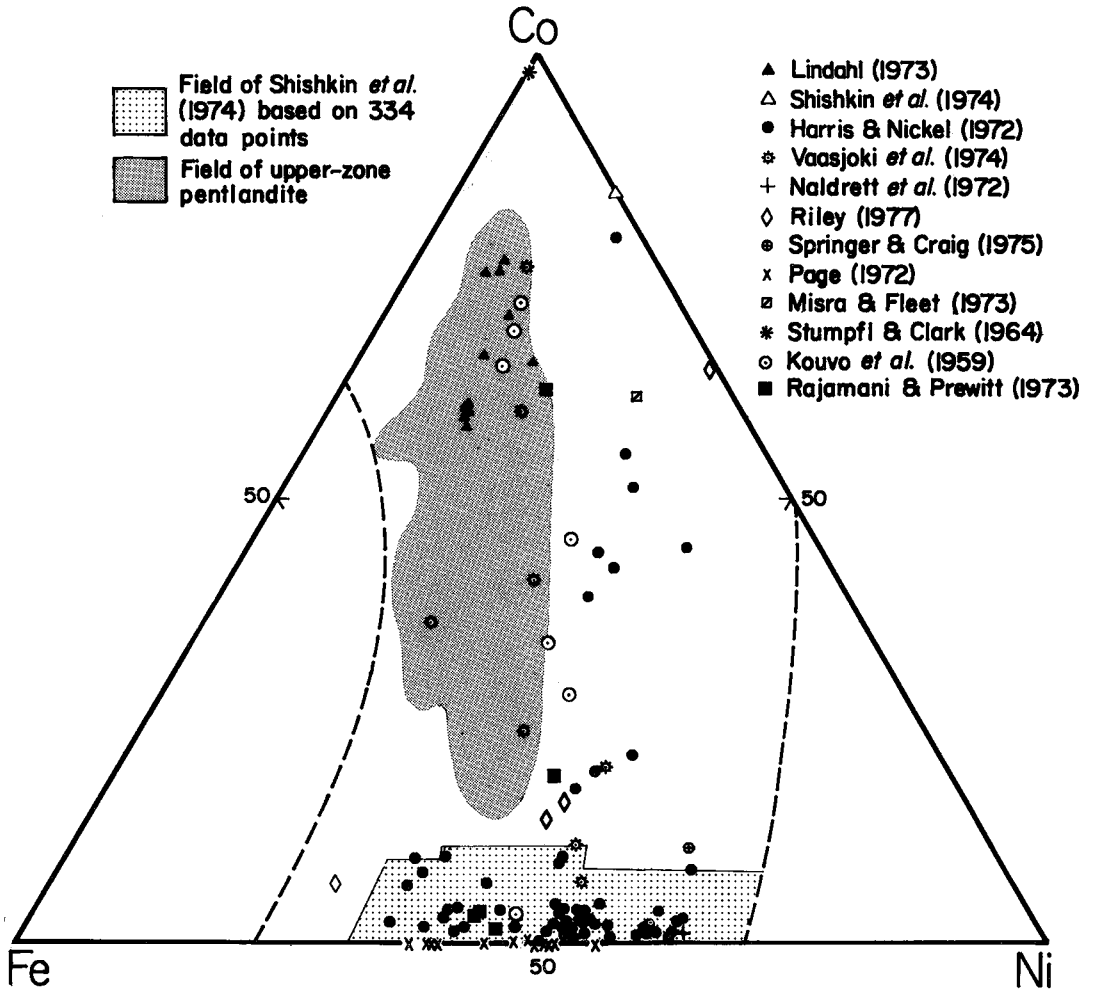


FIG. 6. Field of upper-zone pentlandite (shaded area) and projection points of selected pentlandite data from the literature in the Fe-Co-Ni cation plot. The stippled lines give the limits of known compositions of pentlandite, after Knop & Ibrahim (1961).

gaps in the documentation of values of Co/Ni ratio in pyrrhotite could not be avoided. The small number of compositions do, however, show strong similarities in the trends of Co/Ni in pentlandite and in pyrrhotite.

Except for one sample at a depth of 1112.7 m, which for no obvious reason does not follow the general trend, the pyrrhotite in samples overlying the layers of magnetite is enriched in iron. With increasing distance above layers of magnetite, the average content of iron decreases but increases again significantly above the next layer of magnetite. This pattern is best developed above the two magnetite layers at depth 783.8 and 823.0 m.

Olivine: Results of microprobe analyses show that

the composition of olivine is, with one exception, very constant on the scale of a thin section. Analyses of large grains of olivine (about 1 mm) reveal no compositional inhomogeneity or zonation that exceeds the analytical uncertainty. Large grains of cumulus olivine are chemically indistinguishable from interstitial olivine in the same section. The cobalt content of olivine is generally in the range of 400 to 700 ppm (Fig. 4), whereas the nickel content is always below the detection limit (160 ppm: Table 5).

The atomic ratio Mg/(Mg + Fe) is low and varies between 0.11 and 0.29 in the stratigraphic interval presented here. These extreme values were found at depths of 1112.7 and 1103.7 m, respectively (Fig. 4),

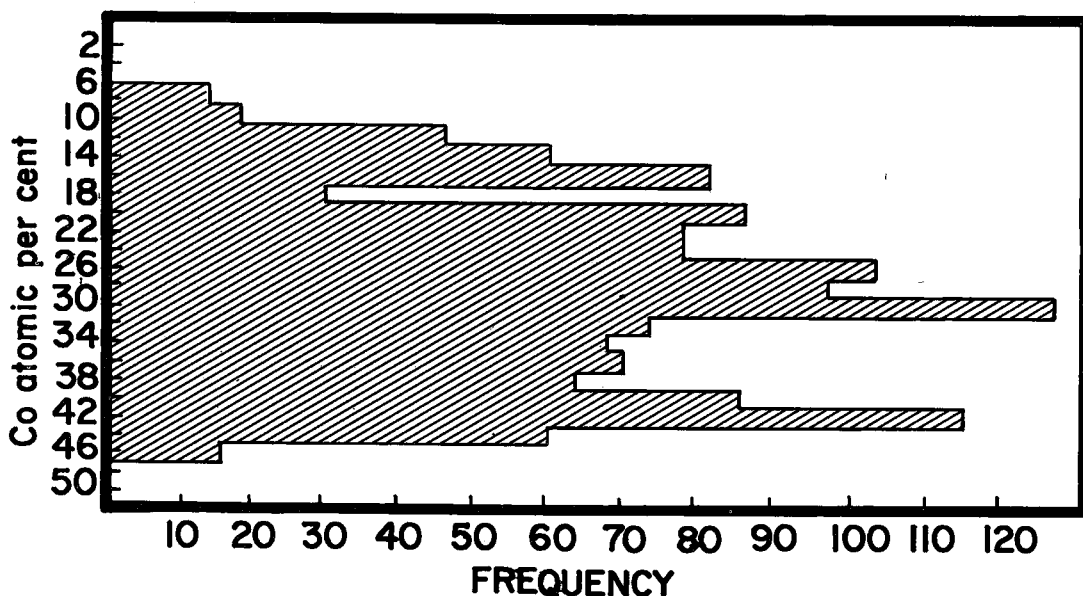


FIG. 7. Frequency distribution of Co contents in upper-zone pentlandite.

where an abrupt reversal in olivine composition appears slightly above the 6-cm-thick layer of magnetite at 1117 m. Below this reversal in the Mg/(Mg + Fe) ratio, olivine follows a strong upward iron-enrichment trend. Above the reversal the magnesium content declines rapidly from about 12% MgO to slightly more than 6% at about 50 m above the reversal. Olivine with a slightly higher magnesium content occurs at higher stratigraphic levels, but the density of olivine sampling does not allow localization of any possible sharp or gradational reversals. Despite the large scatter in cobalt content of the olivine grains analyzed, a vague relation to the Mg/(Mg + Fe) ratio is indicated (Fig. 4). However, the most iron-enriched olivine is from a sample about 2 m above the layer of magnetite at 1117 m. This is explained as being due to a process of infiltration metasomatism (Irvine 1980).

Whole-rock chemistry

If the slight variation in the sulfur content of pyrrhotite and the other minor sulfides is ignored, the bulk content of sulfur of the upper zone can be taken as being proportional to the modal content of sulfides. The sulfur determinations cover the BK-1 core in great detail, with sample spacing in some parts

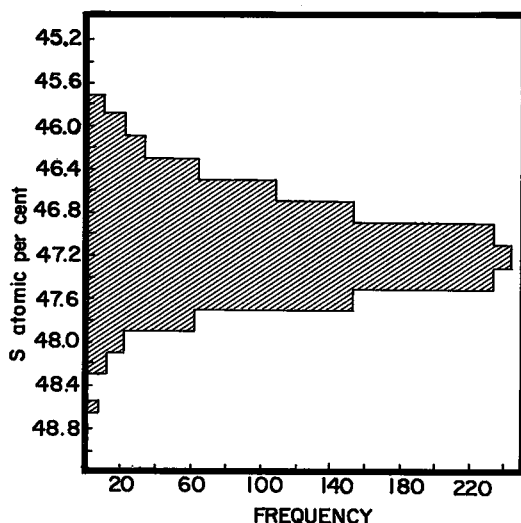


FIG. 8. Frequency distribution of sulfur contents of upper zone pentlandite. The theoretical value is 47.06 atomic %.

TABLE 3. SPEARMAN CORRELATION MATRIX FOR 1306 PENTLANDITE COMPOSITIONS

	Ni	Cu	Fe	S	Fe/Ni	Co/Ni	Fe/Co
Co	-0.9619 0.0001	-0.0607 0.0283	-0.9620 0.0001	0.0831 0.0027	0.7154 0.0001	0.9831 0.0001	-0.9908 0.0001
Ni		0.0032 0.9079	0.8653 0.0001	-0.2021 0.0001	-0.8515 0.0001	-0.9933 0.0001	0.9242 0.0001
Cu			0.0997 0.0003	0.1095 0.0001	0.0335 0.2268	-0.0233 0.3993	0.0837 0.0025
Fe				-0.0424 0.1255	-0.5298 0.0001	-0.9066 0.0001	0.9889 0.0001
S					0.2555 0.0001	0.1565 0.0001	-0.0664 0.0163
Fe/Ni						0.8012 0.0001	-0.6343 0.0001
Co/Ni							-0.9547 0.0001

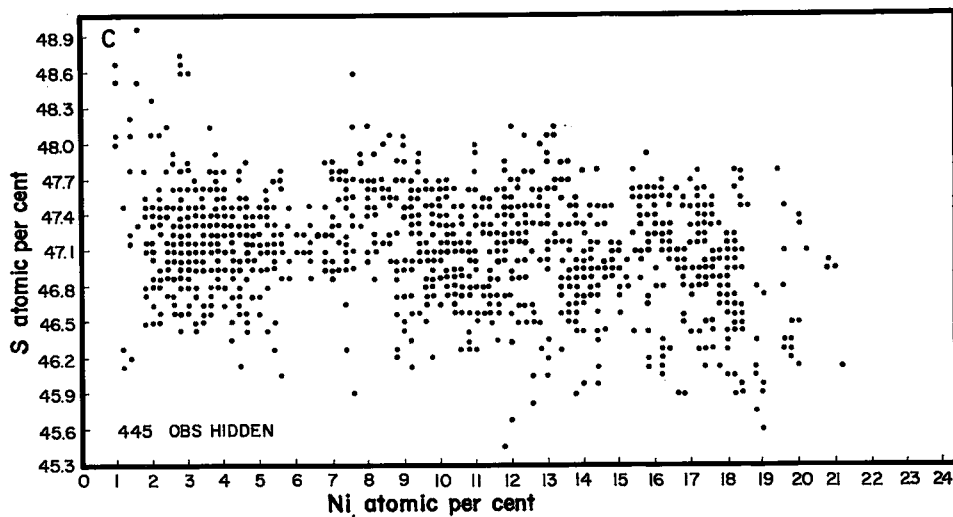
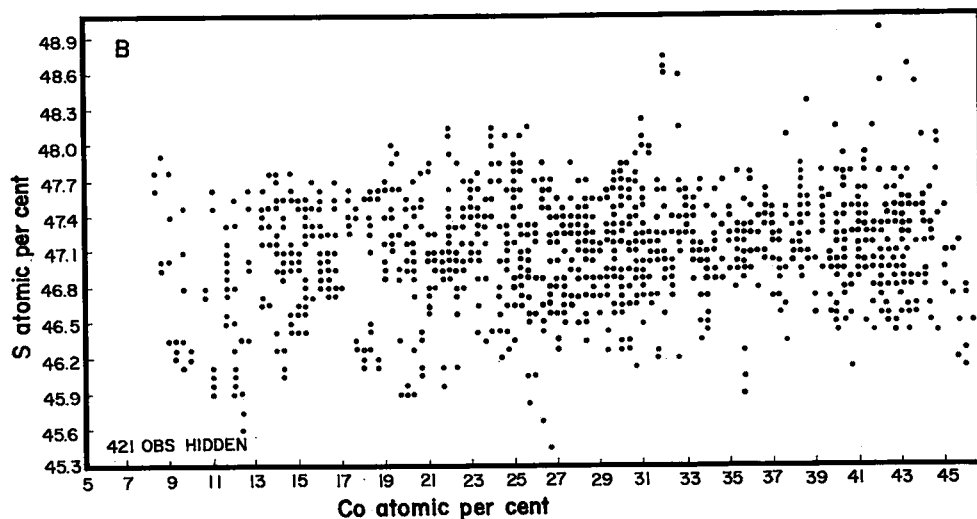
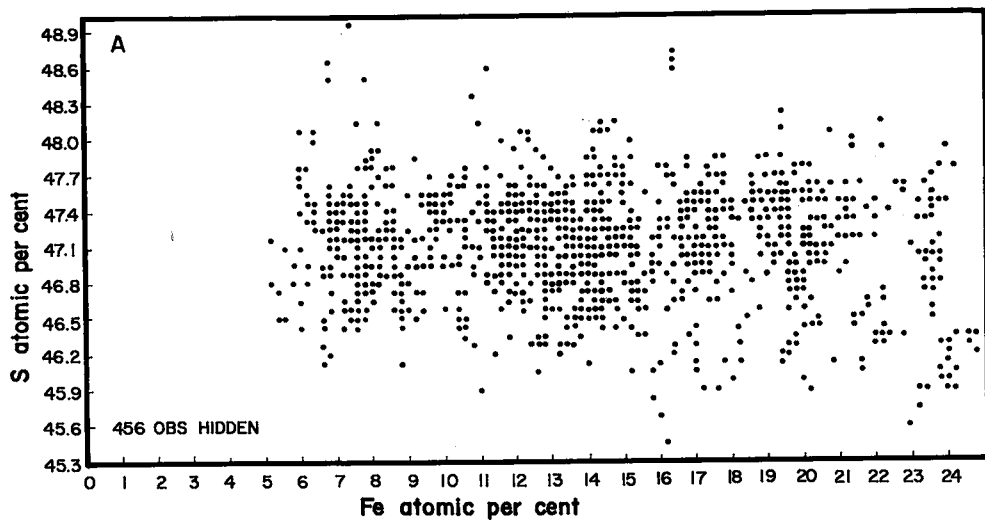


FIG. 9. Unsystematic variation of sulfur in pentlandite as a function of Fe (A), Co (B), and Ni content (C) (in atomic %).

TABLE 4. SELECTED COMPOSITIONS (wt.%) OF PYRRHOTITE COEXISTING WITH PENTLANDITE AT DEPTH 1009.6 m

S	Fe	Ni	Co	Total
38.89	60.60	0.064	0.122	99.68
38.90	60.98	0.058	0.109	100.05
38.53	61.12	0.066	0.106	99.82
38.37	61.60	0.064	0.108	100.14
37.84	62.21	0.059	0.081	100.19
37.84	62.36	0.047*	0.101	100.35
36.73	62.81	0.004*	0.114	99.66
36.38	63.09	0.005*	0.080	99.56
36.78	63.39	0.031*	0.076	100.28
36.74	63.63	0.000*	0.091	100.46

* below detection limit.

as small as 2 metres. The sulfur content in these rocks varies considerably over short distances (Fig. 10). Despite the small-scale variation, however, a roughly cyclic distribution of the sulfur contents in the core is indicated. This cyclic pattern is more clearly visible in parts of the core with higher frequency of samples. It is difficult to clearly define the sizes of these cycles from sulfur data alone, but rapid increase of sulfur content from less than 200 ppm to about 2000 ppm or more could be taken as the base of a sulfur cycle, as is the case at drilling depths 445, 638, 846, 1112, 1494 and 1613 m. Within every one of these cycles, fluctuations in the sulfur content may indicate superimposed smaller cycles. It should also be pointed out that layers of magnetite or rock units with increased magnetite content, tend to coincide with the inferred base of the sulfur cycles. However, where many layers of magnetite occur close together, e.g., between 784 and 893 m, no clear cycles are developed. Many of the other elements that could be analyzed with sufficient accuracy show cyclic patterns that coincide with the sulfur cycles. For some elements, however, a general increase toward the top of the complex is superimposed on these cycles.

According to the Spearman correlation matrix (Table 6), four major groups of elements show com-

parable behavior throughout the investigated part of the upper zone. These groups are: 1) Si, Al, Ca, Na, K, Ba, Rb and Sr, 2) Fe, Ti, Mn, Nb, Zn and Zr, 3) P and Y, and 4) S, Co, Cu and Ni.

Elements of group 1 obviously reflect the silicate component in the rock; they correlate negatively with most of the elements of group 2, which include the components of titaniferous magnetite. Phosphorus reflects the apatite content of the rock. The correlation between P and Y suggests that Y has a high affinity for apatite, a relationship also found by Towell *et al.* (1965). Group 4 represents the sulfide portion of the rock. The elements of this group closely correlate with those elements incorporated in magnetite and therefore are also negatively correlated with the first group. Zirconium not only correlates with the elements of the magnetite and, therefore, also the sulfide group, but also with Mo. Molybdenum is present in the rocks as molybdenite, but does not follow the general sulfide trend. It is enriched in the course of differentiation; its positive correlation with Ba, Nb, Rb, Zn and Zr reflects the similarities in their enrichment trends toward the top of the Bushveld, irrespective of cyclic patterns at lower stratigraphic levels. Yttrium shows an enrichment in the uppermost part as well, but the affinity with apatite is too pronounced to allow a strong correlation coefficient with Mo.

The elements of the sulfide group also correlate with Mg. As the Mg content in the silicates is a measure of the degree of fractionation, similarity to the trends of sulfur in the cycles implies that sulfur and magnesium were replenished in the magma by the same process.

The variation of some elements with height in the BK-1 core is presented in Figure 10. The variation of the Sr contents is given as an example of the behavior of a group-1 component, whereas Ti represents the elements incorporated in magnetite. Phosphorus and yttrium are presented to show the

TABLE 5. REPRESENTATIVE COMPOSITIONS OF OLIVINE FROM SELECTED SAMPLES THAT COVER THE OBSERVED RANGE OF Mg/(Mg + Fe) VALUES

Depth m		772.2	899	940.1	1019.8	1050.2	1068.9	1086.7	1103.7	1128.7
SiO ₂	wt. %	30.44	30.19	30.41	29.26	29.25	30.78	30.19	30.93	30.09
	FeO	59.75	59.42	61.70	63.19	63.30	60.95	58.60	56.10	61.67
MgO		8.35	9.15	6.44	5.85	6.16	7.58	9.33	11.91	7.12
MnO		0.92	1.01	1.08	1.11	1.05	0.95	0.99	0.86	1.03
CaO		0.08	0.03	0.00	0.01	0.00	0.06	0.07	0.10	0.01
TiO ₂		0.00	0.02	0.01	0.01	0.00	0.07	0.00	0.00	0.00
Total		99.54	99.82	99.64	99.43	100.03	100.39	99.18	99.90	99.92
Ni	ppm									
Co		610	690	730	470	590	560	460	320	660
CATIONS ON THE BASIS OF 4 OXYGEN ATOMS										
Si		0.98	0.97	0.99	0.97	0.97	0.99	0.97	0.97	0.98
Fe		1.60	1.60	1.68	1.75	1.73	1.63	1.58	1.47	1.67
Mg		0.41	0.44	0.31	0.29	0.30	0.36	0.45	0.56	0.34
Mn		0.02	0.03	0.03	0.03	0.03	0.03	0.03	0.02	0.03
Mg/(Mg+Fe)		0.205	0.215	0.157	0.142	0.148	0.182	0.221	0.274	0.171

* total iron as FeO.

TABLE 6. SPEARMAN CORRELATION MATRIX FOR WHOLE-ROCK COMPOSITIONS OF UPPER-ZONE ROCKS

	TiO ₂	Al ₂ O ₃	Fe ₂ O ₃	MnO	MgO	CaO	Mg ₂ O	K ₂ O	P ₂ O ₅	S	Ba	Co	Cu	Ni	Nb	Na	Ni	Rb	Sr	Y	Zn	Zr	
SiO ₂	-0.02638 0.0001	0.79776 0.0001	-0.08645 0.0001	-0.43574 0.0001	-0.45055 0.0001	0.21473 0.0114	0.08278 0.3344	0.79226 0.0001	-0.43400 0.0001	-0.08538 0.0001	0.62703 0.0001	-0.08680 0.0001	-0.52714 0.0001	-0.12959 0.0001	-0.32328 0.0002	-0.71565 0.0001	0.54095 0.0001	0.79495 0.0001	-0.26301 0.0024	-0.59242 0.0001	-0.37926 0.0001		
TiO ₂		-0.62791 0.0001	-0.08645 0.0001	-0.43574 0.0001	-0.45055 0.0001	0.21473 0.0114	0.08278 0.3344	0.79226 0.0001	-0.43400 0.0001	-0.08538 0.0001	0.62703 0.0001	-0.08680 0.0001	-0.52714 0.0001	-0.12959 0.0001	-0.32328 0.0002	-0.71565 0.0001	0.54095 0.0001	0.79495 0.0001	-0.26301 0.0024	-0.59242 0.0001	-0.37926 0.0001		
Al ₂ O ₃			-0.91536 0.0001	-0.42457 0.0001	-0.42457 0.0001	0.16433 0.0541	0.29070 0.0005	0.53589 0.0001	-0.44359 0.0001	-0.70465 0.0001	0.49243 0.0001	-0.80555 0.0001	-0.44779 0.0001	-0.19398 0.0001	-0.48298 0.0001	-0.66076 0.0001	0.39436 0.0001	0.91746 0.0001	-0.46236 0.0001	-0.62532 0.0001	-0.70576 0.0001		
Fe ₂ O ₃				-0.74050 0.0001	-0.70682 0.0001	-0.29451 0.0005	-0.25860 0.0022	-0.70069 0.0001	-0.42534 0.0001	-0.60040 0.0001	-0.60040 0.0001	-0.89773 0.0001	-0.47018 0.0001	-0.11792 0.0001	-0.42156 0.0001	-0.69797 0.0001	-0.51382 0.0001	-0.68914 0.0001	-0.64303 0.0001	-0.36966 0.0001	0.72253 0.0001		
MnO					0.00773 0.0073	-0.23201 0.0062	-0.49376 0.0001	-0.29028 0.0005	-0.44326 0.0001	-0.50680 0.0001	-0.40876 0.0001	-0.55342 0.0001	0.20132 0.0001	0.12714 0.0001	0.40132 0.0001	0.43205 0.0001	-0.26947 0.0001	-0.64303 0.0001	-0.53709 0.0001	-0.59358 0.0001	0.46643 0.0001		
MgO						0.05294 0.0001	-0.39434 0.0001	-0.59545 0.0001	-0.33949 0.0001	0.40070 0.0001	-0.67106 0.0001	-0.56429 0.0001	-0.36670 0.0001	-0.02813 0.0001	-0.06224 0.0001	-0.45450 0.0001	-0.45450 0.0001	-0.50091 0.0001	-0.50091 0.0001	-0.25492 0.0001	0.22833 0.0001		
CaO							0.18112 0.0035	0.13948 0.1053	0.38920 0.0001	-0.03792 0.0001	0.19347 0.0001	-0.31446 0.0001	0.05932 0.0001	0.04450 0.0001	0.04450 0.0001	0.27430 0.0001	0.28018 0.0001	0.20200 0.0001	0.36440 0.0001	-0.25581 0.0001	0.22833 0.0001		
Mg ₂ O								0.04298 0.0093	-0.18225 0.0001	-0.27472 0.0001	0.32944 0.0001	-0.29807 0.0008	-0.19042 0.0001	-0.08381 0.0001	-0.02210 0.0001	-0.22180 0.0001	0.15351 0.0001	0.33452 0.0001	-0.30467 0.0001	-0.22775 0.0001	0.1154 0.0001		
K ₂ O									-0.12219 0.0001	-0.52943 0.0001	0.73950 0.0001	-0.02530 0.0001	-0.05659 0.0001	0.00753 0.0001	-0.07948 0.0001	-0.60361 0.0001	0.74227 0.0001	-0.22372 0.0001	-0.05242 0.0001	-0.47175 0.0001	-0.07113 0.0001		
P ₂ O ₅										0.55949 0.0001	-0.30656 0.0004	0.61966 0.0004	0.20102 0.0003	0.13118 0.0003	0.12954 0.0004	0.14600 0.0002	0.25891 0.0001	-0.07231 0.0001	-0.31382 0.0003	0.86273 0.0001	0.30482 0.0004	0.19540 0.0003	
S											-0.36053 0.0001	-0.71474 0.0001	-0.29751 0.0001	0.03887 0.0001	0.47875 0.0001	-0.53348 0.0001	0.84850 0.0001	0.52557 0.0001	0.17280 0.0648	0.62554 0.3553	0.65644 0.0001	0.27979 0.0001	
Ba																							
Co																							
Cu																							
Ni																							
Nb																							
Na																							
K																							
Rb																							
Sr																							
Y																							
Zn																							

The computed level of significance (given underneath the correlation coefficient) is based on 139 cases for major elements, on 131 cases for correlations between trace elements and major elements, and on 217 cases for correlations between trace elements.

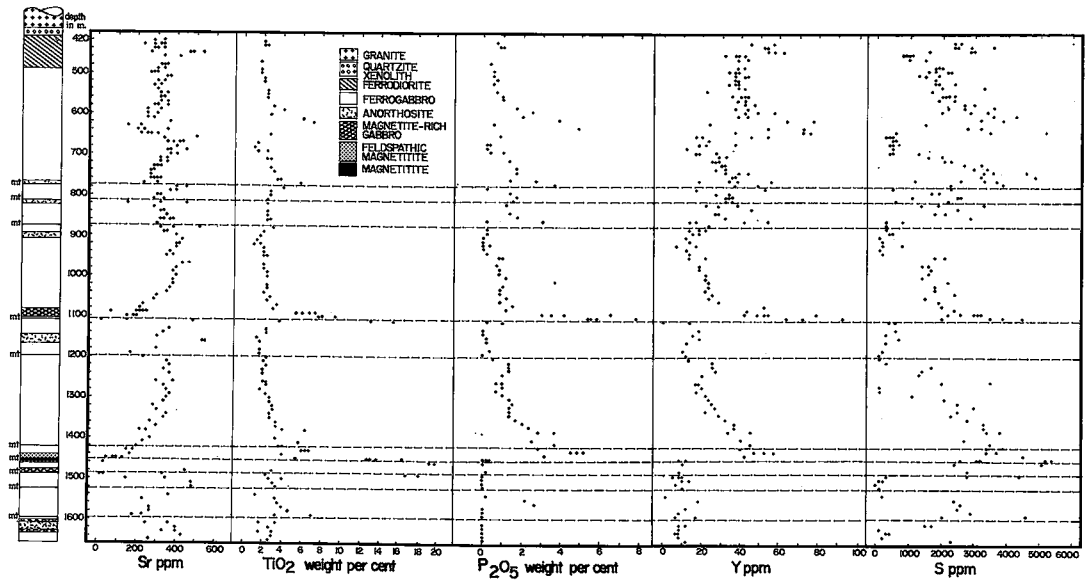


FIG. 10. Variation in whole-rock contents of selected elements in the BK-1 drill core. See text for discussion.

close link between apatite and the concentrations of generally incompatible elements. The four elements of the sulfide group (S, Co, Cu, Ni) are shown in Figure 11.

DISCUSSION

Differentiation in a magmatic body has a signifi-

cant influence on sulfide bulk-composition, which in turn is reflected, firstly, in different assemblages of sulfides at different levels of the complex and, secondly, in the compositional changes of individual sulfide minerals with an extended solid-solution range. In the upper zone at Bierkraal, olivine fractionated throughout the larger part of the sequence. At the same time, the melt was constantly unmixing

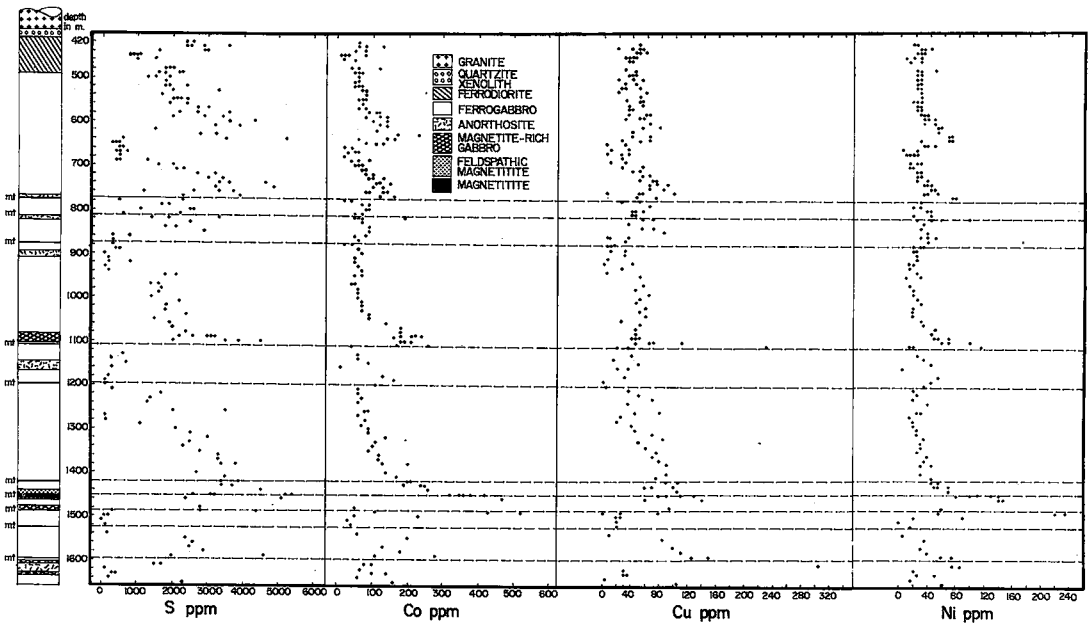


FIG. 11. Variation in whole-rock contents of sulfur, cobalt, copper and nickel in the BK-1 drill core.

small amounts of immiscible sulfide melt. Both factors resulted in a more rapid depletion of Ni compared to Co, because for both olivine and a sulfide melt, Ni has a higher distribution-coefficient than Co (Irving 1978, MacLean & Shimazaki 1976). This combined effect increased the bulk Co/Ni ratio of the magma and in the separated sulfide liquid rapidly during differentiation. Ni and Co in the sulfide melt will largely exsolve from the monosulfide solid-solution to form pentlandite upon cooling, and this mineral should therefore largely reflect the changes in bulk Co/Ni ratio in the magma.

The pattern that one would expect to find reflected in pentlandite composition is a smooth trend of increasing Co/Ni ratio toward the roof of the Bushveld. This is, however, not the case, and the reason for the development of patterns such as those depicted in Figure 3 is considered to reflect a combination of repeated replenishment of the crystallizing melt by mixing with less evolved magma (see below) and the amount of sulfide formation shortly after replenishment. Unmixing of a sulfide liquid results in a depletion of both Ni and Co in the silicate melt according to their distribution coefficients. Ni decreases more rapidly than Co and will reach such a low level that complete equilibrium with the separating sulfide melt will not always be achieved. Co will then be depleted from the silicate liquid more

rapidly than Ni, so that the Co/Ni ratio in the immiscible sulfide melt will tend to decrease. Close to the base of the cycles a comparably large volume of sulfide melt separates, so that the Co/Ni ratio changes rapidly over a short stratigraphic interval. During the evolution of the cycle, the amount of immiscible sulfide melt declines, and the trend of the declining Co/Ni ratio is slowed down and stretches over a larger stratigraphic interval.

The Co/Ni trends in pentlandite, in pyrrhotite, and in the whole-rock composition are quite similar (Figs. 3, 4). In Figure 12 the average Co/Ni values in intermediate pyrrhotite and in the coexisting pentlandite are plotted against each other. Up to a ratio of about 4 in pyrrhotite, the projection points scatter around a 1:1 ratio, whereas the pentlandite becomes more Co-enriched at higher Co/Ni values in pyrrhotite. Careful examination of the analytical results discloses that high Co/Ni values in intermediate pyrrhotite are caused by a lower Ni rather than a higher Co content, compared to intermediate pyrrhotite with lower values. Higher analytical error at lower concentrations may cause calculation of incorrect values of the Co/Ni ratio, although purely analytical error can hardly explain the change of the observed trend. Because the values plotted are averages of a number of analyses per sample, and because Co/Ni values could only be calculated for analyses with sufficiently high values of Ni, the averages are biased toward lower values of the Co/Ni ratio in these samples, which contain a high proportion of

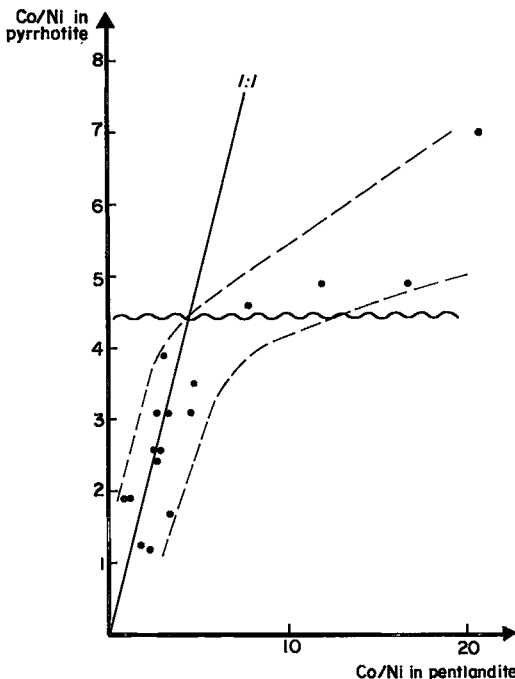


FIG. 12. Relation between the atomic Co/Ni ratio in coexisting pyrrhotite and pentlandite. See text for discussion.

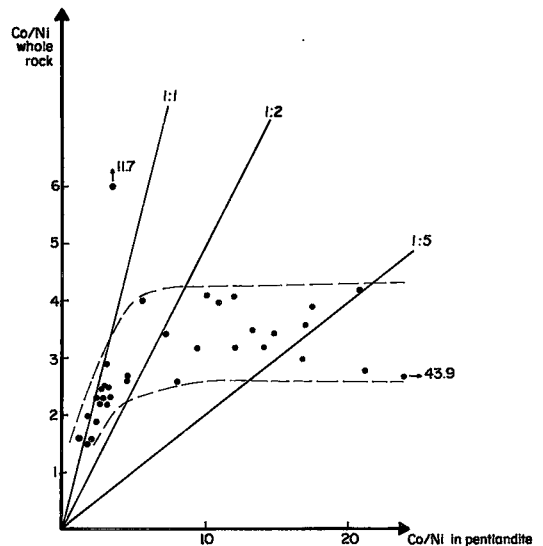


FIG. 13. Co/Ni ratio in whole rock and its relation to the Co/Ni atomic ratio in pentlandite. The nonlinear trend reflects differences between the samples in the timing of the separation of the immiscible sulfide melt from the silicate melt (see text).

intermediate pyrrhotite with a Co/Ni ratio of higher than 4.

A similar problem of nonlinearity exists between Co/Ni in whole rocks and in pentlandite (Fig. 13). A fairly constant relation of about 1:1 to 1:2 at a low ratio changes to much higher values of the Co/Ni ratio in pentlandite at a Co/Ni ratio of about 2.5 and higher in bulk composition. Faulty analyses can be ruled out as a reason for this trend, because re-analysis of some samples showed the results to be reliable.

As already mentioned, the distribution coefficients dictate that a higher proportion of whole-rock Ni than of Co is expected to have partitioned into the immiscible sulfide. Furthermore, the amount of Ni tolerated in the pyrrhotite structure at low temperatures is smaller than the amount of Co. Therefore it should be expected that any difference in Co/Ni ratio between whole rock and pentlandite would be caused by a lower Co/Ni ratio in pentlandite. According to Figure 13, however, Co/Ni in pentlandite is higher if the whole-rock ratio increases. In this diagram, mean values are plotted, so that the secondary process discussed below, which can result in higher values of the Co/Ni ratio in individual grains of pentlandite, has no effect on the graphical presentation.

This discrepancy is therefore interpreted to reflect a primary compositional feature of the sulfide melt. The difference in Co/Ni between the whole rock and the sulfide melt can become quite substantial if the sulfide melt separates after a large amount of silicates (*e.g.*, olivine, for which Ni has a high affinity) have already crystallized. This results in a depletion of Ni relative to Co on a very small scale, and the sulfide melt separating from such a silicate melt will not be in equilibrium with the whole rock as we see it today.

The total variation of the Co contents in specific samples is shown in Figure 3. The large spread indicates that the pentlandite in the upper zone is not homogeneous at a thin-section scale. A possible explanation for these variations could be that different particles of sulfide melt unmixed at slightly different times from the same volume of magma. Whereas some might have been in contact with the overlying pile of magma (Tait *et al.* 1984), others might have been trapped with (or separated from) intercumulus melt and represent an internal trend of differentiation on a sample scale. Solid-state diffusion from adjacent oxides and silicates seems to have influenced the Co and Ni concentrations in the sulfide particles, and differences in the proportions and types of the adjoining minerals affected the Ni/Co ratio of every sulfide particle differently. In addition, infiltration metasomatism (Irvine 1980) and hydrothermal fluids could have changed the composition of pyrrhotite and possibly also of olivine

overlying the layers of magnetite (see below), and may have redistributed the Co content on a millimetre scale. The large number of data used to calculate the arithmetic mean, however, should compensate for this scatter.

The reversal in Mg/(Mg + Fe) ratio of olivine shows that between the drilling depths 1103.7 and 1112.7 m, an event of rapid mixing has taken place in the upper-zone magma, resulting in a significant increase of the Mg content in the melt. Excluding sample 1112.7 because of probable effects of infiltration metasomatism, the Mg content in olivine increases by about 5 weight % MgO from slightly more than 7 to 12 weight %. The partition coefficient of Mg for olivine in such an iron-rich environment might differ from that in a magnesium-rich environment, but to cause such an abrupt change in olivine composition, the Mg content of the melt must have been increased in the order of 1 to 2 weight % MgO. However, through differentiation and crystallization of only about 50 m of rock, the bulk composition of the melt returned to a comparable composition prior to the reversal in terms of its magnesium content. This strong differentiation over such a short distance shows that strong fractionation involved a small volume of magma and, therefore, an even smaller volume of less-evolved melt was involved in the mixing event.

The cobalt content of olivine is much higher than its Ni content, indicating a very high Co/Ni ratio in the melt at this level of the upper zone. Even after the increase in magnesium content, nickel is still not detectable with the microprobe. The distribution coefficient of Ni for olivine is high, even if sulfides form at the same time (*e.g.*, Rajamani & Naldrett 1978), and is assumed here not to deviate very much in very iron-rich melts. The low Ni content of the olivine also indicates that the magma mixing did not involve a new pulse of magma. The variation of the Co content in olivine is thought to reflect the interaction between concentration during silicate formation and depletion of Co in the melt due to separation of an immiscible sulfide melt.

At the stratigraphic interval discussed here in detail and between 1422 and 1198 m it is possible to demonstrate the relation between the beginning of the sulfur cycles and other geochemical cycles. An increase in the sulfur content at about 900 m (Fig. 10) concomitant with an increase in the magnesium content of olivine (Fig. 4) may indicate another mixing event. Whether a gradational mixing took place, as may be deduced from the sulfur content, or whether a rapid-mixing occurred cannot be inferred with our present knowledge.

The cyclicity of elements in the upper-zone rocks and the close relation of most of the recognized cycles to layers of magnetite strongly indicate that the formation of layers of magnetite and of sulfur-enriched

horizons in the upper zone are genetically linked. The sulfur cycles themselves are often not as smooth as the trends of the other elements. This is believed to be due to a complex interaction of processes. On the one hand, differentiation (*i.e.*, crystallization of silicates) will concentrate sulfur if the magma has not yet reached saturation; on the other hand, differentiation can cause a reduction of sulfur solubility in the melt if the activity of iron or silica changes. The chalcophile elements will become depleted with the separation of sulfide melt, and differences in their distribution coefficients will cause depletion to varying degrees. This, for example, can lead to changes in the Co/Ni ratio and the composition of the pentlandite.

As mentioned earlier, the layers of magnetite in the upper zone tend to be associated with higher modal proportions of chalcopyrite. Higher proportions of Cu in the immiscible sulfide melt can have three possible causes:

- 1) The silicate melt from which the sulfide melt separates has a higher Cu content, or
- 2) the sulfide melt equilibrated with a larger amount of silicate melt [higher R-factor (Campbell & Naldrett 1979)] and in that way extracted more Cu, or
- 3) the distribution coefficient is affected by changes in the Mg content of the melt.

If we assume that within any one convection cell in the upper-zone magma the melt was close to sulfur saturation (as is indicated by the common sulfide inclusions in silicates), copper should become rapidly depleted because of its high distribution-coefficient (50 or more: MacLean & Shimazaki 1976, Rajamani & Naldrett 1978). A sudden change in intensive parameters (*e.g.*, oxygen fugacity) to form monomineralic layers of magnetite will have no effect on the copper content in the immiscible sulfide melt, which might form as a result of the reduced content of iron and therefore reduced solubility of sulfur. To increase the copper content, a mixing event has to take place, either by adding magma (*i.e.*, less evolved magma or less depleted in Cu) to the crystallizing part of the magma chamber or by allowing the unmixing sulfide droplets to extract copper from a larger volume of magma. The same applies to the contents of all chalcophile elements.

The small amount of magma involved in the reversal described at about 1117 m and the low contents of Cu (maximum value 240 ppm at a sulfur value of about 0.45 weight %) at this level do not speak in favor of addition of new magma. They rather indicate mixing as an effect of the breakdown of a convection cell. This does not, however, rule out the possibility that thicker layers of magnetite at lower stratigraphic levels of the upper zone were formed by the effect of magma addition.

Consequently, the higher S, Cu, Co and Ni concentrations in the rocks at the base of the cycle

between 875 and 1117 m are not merely due to an increase in the modal proportions of sulfides, but reflect a change in the composition of the crystallizing magma. This change affected not only the Mg/(Mg + Fe) ratio of the olivine but also the Co content and the Co/Ni ratio in the base-metal sulfides.

CONCLUSIONS

The results from the upper zone of the western Bushveld at Bierkraal show that:

1. Cobalt-rich pentlandite can be a primary magmatic mineral, which can exsolve from an immiscible sulfide melt on cooling, if the silicate melt was highly evolved and depleted in Ni.
2. Individual pentlandite grains are not necessarily stoichiometric. On average, however, they closely approach the formula Me_9S_8 . There is no indication of a systematic relationship between deviation from stoichiometry and metal contents or metal ratios.
3. The Co/Ni ratio in pentlandite is matched by the Co/Ni ratio in coexisting intermediate pyrrhotite.
4. The Co/Ni ratio in pentlandite corresponds to the Co/Ni ratio in the whole rocks if the sulfide melt separated after only a small proportion of the rock was solidified.
5. The upper zone of the western Bushveld Complex does not represent products of uninterrupted differentiation of a homogeneous melt. Several cycles of differentiation are reflected in the whole-rock geochemistry, especially in the content of chalcophile elements and sulfur, but also in the concentration of incompatible elements. In addition, these cycles are reflected in the composition of pentlandite and of olivine.
6. Reversals in olivine composition suggest that the cycles were produced by mixing events, although the magnitude and vertical distribution of reversals in the upper part of the upper zone suggest a periodic breakdown of convection cells as the cause of magma mixing, rather than magma addition at the stratigraphic levels concerned.
7. The high Co and very low Ni contents of olivine above the level of mixing rule out the involvement of an undifferentiated melt. This, however, does not rule out the possibility that thicker cycles lower in the sequence could represent the addition of more primitive magma, although more work is required in this regard.
8. The position of layers of magnetite at the base of clearly defined geochemical cycles strongly indicates a genetic link between the formation of layers of magnetite and magma mixing. It seems, however, that mixing did not always result in the formation of a layer of magnetite.

ACKNOWLEDGEMENTS

We are greatly indebted to the following persons and institutions: the Director of the Geological Survey of South Africa for providing the core for this investigation, Dr. C. Frick for providing certain analytical facilities at the Geological Survey, Dr. R.G. Cawthorn for sharing his powdered samples with us, and M. Potgieter for drafting of the diagrams. Special thanks are due to H. Horsch for her invaluable help with the microprobe work. This report emerged from ongoing research on sulfides in the Bushveld Complex. Financial support by the Foundation for Research Development of the Council for Scientific and Industrial Research of South Africa is gratefully acknowledged. Valuable comments by Dr. R.F. Martin and two reviewers are greatly appreciated.

REFERENCES

- CAMPBELL, I.H. & NALDRETT, A.J. (1979): The influence of silicate:sulfide ratios on the geochemistry of magmatic sulfides. *Econ. Geol.* **74**, 1503-1506.
- DURAZZO, A. & TAYLOR, L.A. (1982): Exsolution in the mss - pentlandite system: textural and genetic implications for Ni-sulfide ores. *Mineral. Deposita* **17**, 313-332.
- HARRIS, D.C. & NICKEL, E.H. (1972): Pentlandite compositions and associations in some mineral deposits. *Can. Mineral.* **11**, 861-878.
- HUHMA, A. & HUHMA, M. (1970): Contribution to the geology and geochemistry of the Outokumpu region. *Geol. Soc. Finland Bull.* **42**, 57-99.
- IRVINE, T.N. (1980): Magmatic infiltration metasomatism, double-diffusive fractional crystallization, and adcumulus growth in the Muskox Intrusion and other layered intrusions. In *Physics of Magmatic Processes* (R.B. Hargraves, ed.). Princeton University Press, Princeton, N.J.
- IRVING, A.J. (1978): A review of experimental studies of crystal/liquid trace element partitioning. *Geochim. Cosmochim. Acta* **42**, 743-770.
- JAROSEWICH, E., NELEN, J.A. & NORBERG, J.A. (1979): Electron microprobe reference samples for mineral analyses. *Smithsonian Contr. Earth Sci.* **22**, 68-72.
- KAISER, H. & SPECKER, H. (1956): Bewertung und Vergleich von Analysenverfahren. *Z. Anal. Chem.* **149**, 46-66.
- KELLY, D.P. & VAUGHAN, D.J. (1983): Pyrrhotine - pentlandite ore textures: a mechanistic approach. *Mineral. Mag.* **47**, 453-463.
- KNOP, O. & IBRAHIM, M.A. (1961): Chalkogenides of the transition elements. II. Existence of the π -phase in the M_9S_8 section of the system Fe-Co-Ni-S. *Can. J. Chem.* **39**, 297-317.
- KOUVO, O., HUHMA, M. & VUORELAINEN, Y. (1959): A natural cobalt analogue of pentlandite. *Amer. Mineral.* **44**, 897-900.
- LINDAHL, I. (1973): Cobalt pentlandite from Kongsfjell, Nordland and Birtavarre, northern Troms. *Norges Geol. Unders.* **294**, 9-19.
- MACLEAN, W.H. & SHIMAZAKI, H. (1976): The partition of Co, Ni, Cu and Zn between sulfide and silicate liquids. *Econ. Geol.* **71**, 1049-1057.
- MISRA, K.C. & FLEET, M.E. (1973): The chemical composition of synthetic and natural pentlandite assemblages. *Econ. Geol.* **68**, 518-539.
- MORIMOTO, N., GYOBU, A., TSUKUMA, K. & KOTO, K. (1975): Superstructure and nonstoichiometry of intermediate pyrrhotite. *Amer. Mineral.* **60**, 240-248.
- NALDRETT, A.J., GASPARRINI, E., BUCHAN, R. & MUIR, J.E. (1972): Godlevskite (β -Ni₇S₈) from the Texmont mine, Ontario. *Can. Mineral.* **11**, 879-885.
- NORRISH, K. & HUTTON, J.T. (1969): An accurate X-ray spectrographic method for the analysis of a wide range of geological samples. *Geochim. Cosmochim. Acta* **33**, 431-453.
- PAGE, N.J. (1972): Pentlandite and pyrrhotite from the Stillwater complex, Montana: iron-nickel ratios as a function of associated minerals. *Econ. Geol.* **67**, 814-818.
- PETRUK, W., HARRIS, D.C. & STEWART, J.M. (1969): Langisite, a new mineral, and the rare minerals cobalt pentlandite, siegenite, parkerite and bravoite from the Langis mine, Cobalt-Gowganda area, Ontario. *Can. Mineral.* **9**, 597-616.
- RAJAMANI, V. & NALDRETT, A.J. (1978): Partitioning of Fe, Co, Ni, and Cu between sulfide liquid and basaltic melt and the composition of Ni-Cu sulfide deposits. *Econ. Geol.* **73**, 82-93.
- _____ & PREWITT, C.T. (1973): Crystal chemistry of natural pentlandites. *Can. Mineral.* **12**, 178-187.
- RILEY, J.F. (1977): The pentlandite group (Fe,Ni,Co)₉S₈: new data and an appraisal of structure-composition relationships. *Mineral. Mag.* **41**, 345-349.
- SACS (1980): Stratigraphy of South Africa. Part 1 (Comp. L.E. Kent) Lithostratigraphy of the Republic of South Africa, South West Africa/Namibia, and the Republics of Bophuthatswana, Transkei and Venda. *Handbook Geol. Surv. S. Afr.* **8**.

- SHISHKIN, N.N., KARPENKOV, A.M., KULAGOV, E.A. & MITENKOV, G.A. (1974): Classification of minerals of the pentlandite group. *Dokl. Acad. Sci. USSR, Earth Sci. Sect.* **217**, 109-111.
- SPRINGER, R.K. & CRAIG, J.R. (1975): Sulfide mineralogy of metamorphosed ultramafic rocks, western Sierra Nevada foothills, California. *Econ. Geol.* **70**, 1478-1483.
- STUMPF, E.F. & CLARK, A.M. (1964): A natural occurrence of Co_9S_8 , identified by X-ray microanalysis. *Neues Jahrb. Mineral. Monatsh.*, 240-245.
- TAIT, S.R., HUPPERT, H.E. & SPARKS, R.S.J. (1984): The role of compositional convection in the formation of adcumulate rocks. *Lithos* **17**, 139-146.
- TOWELL, D.G., WINCHESTER, J.W. & SPIRN, R.V. (1965): Rare earth distributions in some rocks and associated minerals of the batholith of Southern California. *J. Geophys. Res.* **70**, 3485-3496.
- VAAJOKI, O., HÄKLI, T.A. & TONTTI, M. (1974): The effect of cobalt on the thermal stability of pentlandite. *Econ. Geol.* **69**, 549-551.
- VON GRUENEWALDT, G. (1976): Sulfides in the upper zone of the eastern Bushveld Complex. *Econ. Geol.* **71**, 1324-1336.
- WALRAVEN, F. & WOLMARANS, L.G. (1979): Stratigraphy of the upper part of the Rustenburg Layered Suite, Bushveld Complex, in western Transvaal. *Annals. Geol. Surv. S. Afr.* **13**, 109-114.

Received October 16, 1985, revised manuscript accepted February 3, 1986.